

# Prospects of heavy ion fusion in cylindrical geometry

M.M. BASKO, M.D. CHURAZOV, AND A.G. AKSENOV

Institute for Theoretical and Experimental Physics, Moscow, Russian Federation

## Abstract

A possibility is analyzed to use direct drive cylindrical targets in the fast ignition mode irradiated by beams of nearly relativistic heavy ions with long ranges in matter. The minimum beam energy required to compress the DT fuel in a 1-cm-long target to  $(\rho R)_{DT} = 0.5 \text{ g/cm}^2$ ,  $\rho_{DT} = 100 \text{ g/cm}^3$  is found to lie in the range 10–15 MJ. Ignition and axial burn propagation is achieved with a 0.2-ns, 0.4-MJ pulse of 100-GeV heavy ions. Thermonuclear energy gains in the range 50–150 appear to be possible.

**Keywords:** Beam energy; Cylindrical targets; Heavy ion inertial fusion; Thermonuclear energy

## 1. INTRODUCTION

One of the major problems for a heavy ion driver for inertial confinement fusion (ICF) is to provide a high enough irradiation intensity on target. From this viewpoint, it would be advantageous to use ions with nearly relativistic energies of  $E_i \gtrsim 0.5 \text{ GeV/u}$ . However, these ions have such long ranges in matter that it would hardly be possible to accommodate such beams in efficiently performing ICF targets with a spherical geometry of fuel compression. Thus, cylindrical targets with axial beam propagation become a natural option.

Here we discuss several key physics issues for a possible version of such a target driven directly by energetic heavy ions with ranges as long as  $5\text{--}20 \text{ g/cm}^2$ . Efficient target performance is achieved by launching a burn wave along a cylindrical “pencil” of cold compressed DT from one end by a powerful igniting beam of heavy ions. It is known that the critical  $\rho R$  for propagation of a steady-state burn wave along a DT cylinder surrounded by a heavy-metal shell is around  $0.3\text{--}0.4 \text{ g/cm}^2$  (Avrorin *et al.*, 1984). We choose our target to have  $(\rho R)_{DT} = 0.5 \text{ g/cm}^2$  in the compressed state.

The target, shown schematically in Figure 1, is driven by two separate ion pulses: a relatively low-power compression pulse and a high-power ignition pulse. Accordingly, its performance is analyzed in two separate stages: ignition, which is essentially a two-dimensional phenomenon, is simulated with a two-dimensional code, while the stage of compression is investigated with a one-dimensional code.

## 2. FAST IGNITION WITH A HIGH-POWER ION BEAM

Ignition is the most critical issue in the present scheme because it pushes demands on the igniting ion beam to the extreme. We consider ignition of a preassembled configuration consisting of a uniform DT cylinder with  $(\rho R)_{DT} = 0.5 \text{ g/cm}^2$ , surrounded by a massive shell (tamper) of heavy metal in pressure equilibrium with the compressed DT. The main role of the tamper is to provide a longer confinement time, which enables fast ignition with the lowest possible beam power. Also, once ignited, a heavy-metal tamper raises the burn fraction of the DT fuel to  $f_b \approx 0.4\text{--}0.6$ . We choose the density of the compressed DT to be  $\rho_{DT} = 100 \text{ g/cm}^3$ , which corresponds to  $R_{DT} = 50 \text{ }\mu\text{m}$  and  $dM_{DT}/dz = \pi\rho_{DT}R_{DT}^2 = 8 \text{ mg/cm}$ . The chosen DT density (for a given  $\rho_{DT}$  value) is already high enough to result in a tolerable level of the thermonuclear yield of  $dY/dz = 340 \text{ [MJ/mg]}$   $f_b dM_{DT}/dz \lesssim 1.5 \text{ GJ/cm}$ , but still not too high to lead to unrealistic demands on the intensity of the igniting ion beam.

We assume that the DT cylinder is ignited from one end by a pulse of heavy ions with the focal spot radius of  $r_{foc} = R_{DT} = 50 \text{ }\mu\text{m}$  and the range of  $(\rho l)_{b,DT} = 6 \text{ g/cm}^2$ —which, in particular, would be the range of 100 GeV Bi ions in cold DT at  $\rho_{DT} = 100 \text{ g/cm}^3$ . One easily estimates that we need  $\geq 300 \text{ kJ}$  to heat up the DT mass  $\Delta M_{DT} = \pi R_{DT}^2 (\rho l)_{b,DT} \approx 0.47 \text{ mg}$  to the ignition temperature  $T \geq 5 \text{ keV}$ . Two-dimensional simulations performed independently with the Eulerian three-temperature (3T) code MDMT (Churazov *et al.*, 2001) at the Institute of Theoretical and Experimental Physics, and with the MIMOZA-ND code (Vatulin *et al.*, 2002) at the Russian Federal Nuclear Center VNIIEF, have shown that ignition and burn propagation are achieved with

Address correspondence and reprint requests to: M.M. Basko, ITEP, B. Chermushkinskaya 25, 117259 Moscow, Russia. E-mail: basko@vitep1.itep.ru

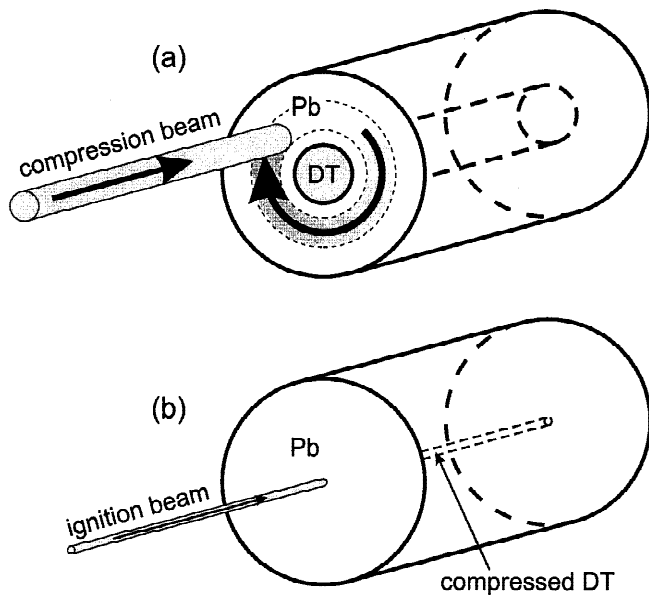


**Fig. 1.** Schematic view of the investigated cylindrical target in its initial state (a), and in the state of maximum compression (b).

the beam energy  $E_{igb} = 400$  kJ delivered in a  $t_{igb} = 0.2$ -ns-long pulse.

The evolution of the density and temperature profiles along the axis of the DT cylinder, as calculated with the MDMT code, is shown in Figure 2. In simulations, it was taken into account that the beam energy deposition peaks towards the end of the ion range (the Bragg peak), and that the Bragg peak advances along the mass coordinate in the axial direction as the DT density drops (see Fig. 2a) due to radial expansion of the DT channel. It is seen that during the second half of the pulse, the Bragg peak overtakes and heats up the hump of the density wave launched along the  $z$ -axis—a beneficial two-dimensional effect characteristic of the ignition mode considered here.

Our total power,  $W_{igb} = E_{igb}/t_{igb} = 2$  PW, and the irradiation intensity,  $I_{igb} = W_{igb}/\pi R_{DT}^2 = 2.5 \times 10^{19}$  W/cm<sup>2</sup>, of the igniting beam are quite close to the optimal values calculated by Atzeni (1999) for a cylindrical heated DT volume surrounded by the cold DT with the same density  $\rho_{DT} = 100$  g/cm<sup>3</sup>. However, we achieve ignition at a five times lower specific deposition power,  $q = 10$  PW/mg, in the critical last 10% [ $(\rho\Delta z)_{DT} = 0.6$  g/cm<sup>2</sup>] of the ion range, where some 20% of the beam energy is deposited. The latter is possible due to additional confinement provided by the heavy-metal tamper.

An igniting beam of heavy ions with the above mentioned parameters can be created under the conditions that (1) the ion energy is increased from the conventional 5–10 GeV to  $\approx 100$  GeV per ion, (2) the method of non-Liouvillian compression of beams of simultaneously accelerated ions with four different masses and opposite electric charges is employed, and (3) the neutralization of the electric charge density is achieved by combining the beams of opposite

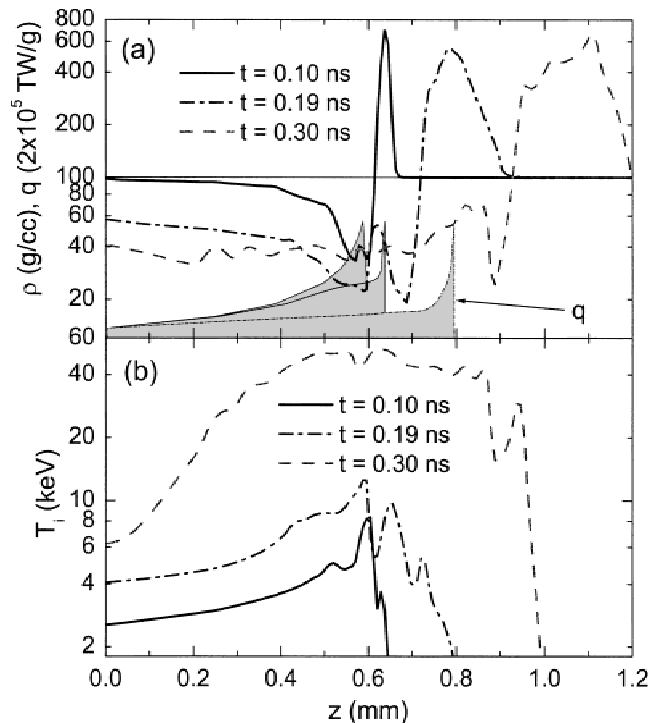


**Fig. 2.** Axial profiles (a) of the density  $\rho$  (curves) and the specific (per unit mass) beam deposition power  $q$  (shaded areas), and (b) of the ion temperature  $T_i$  in the target center at times  $t = 0, 0.10$  ns,  $0.19$  ns, and  $0.30$  ns after the ignition beam is on.

charges at the last stage of beam compression. More details are given in the presentation by D.G. Koshkarev (pers. comm.).

### 3. TARGET COMPRESSION

Tangential (with respect to the accelerated interface) irradiation geometry in cylindrical targets provides an opportunity to ensure a high degree of azimuthal symmetry of the ion energy deposition—an important prerequisite for using direct drive—by fast (with a period of  $\leq 0.1$  ns) rotation of the compression beam around the target axis (see Fig. 1a). Axial uniformity of the ion drive at the stage of compression can be controlled by using subrange targets, which would let the Bragg peak be outside the working target section and utilize only about two-thirds of the initial ion energy, possibly combined with two-sided irradiation and axial shaping of the target structure. Having assumed that the required uniformity of the ion drive is ensured, we can use a one-dimensional code to simulate the compression stage.

On the other hand, tangential irradiation forces us to adopt an implosion strategy which is rather different from the conventional approach. The main harmful effect we have to cope with is the “clearance” of the absorber layer in the process of irradiation by the ion pulse: As the density  $\rho_a$  of the heated absorber drops in the course of its radial expansion, its mass thickness  $\rho_a\Delta z$  in the axial

direction (i.e., along the ion trajectories) decreases in the same proportion. As a result, the fraction of the ion energy left in the target becomes smaller and smaller (we assume that the ion energy is kept fixed during the pulse). Evidently, beam energy losses due to this effect may become prohibitively excessive for thin-shell absorbers. Our principal aim here is to minimize the total energy and the peak power of the compression beam. In practice this means minimizing the entropy of the compressed target core, and minimizing the clearance effect.

Under the direct ion drive, the Rayleigh–Taylor instability of the absorber–pusher (pusher is the imploded cold layer of heavy metal between the absorber and the DT fuel, see Fig. 1a; at stagnation it becomes the tamper) interface becomes an issue. Sufficient stabilization can be achieved by means of a shallow density gradient as described by Basko *et al.* (2002), provided that we avoid initial density jumps. Accordingly, we assume that initially the target consists of a uniform lead (Pb) tube ( $R_{DT,0} < r < R_0$ ), filled with the DT fuel (see Fig. 1a). We found that the best results were obtained when the entire central region  $0 < r < R_{DT,0}$  is filled with the DT ice. Then, for  $\rho_{DT,0} = 0.225 \text{ g/cm}^3$  and the DT mass adopted for ignition, we calculate  $R_{DT,0} = 1.05 \text{ mm}$ . In simulations, we took a somewhat larger value of  $R_{DT,0} = 1.12 \text{ mm}$ . The initial outer radius  $R_0$  was fixed at a reasonably large value of  $R_0 = 4 \text{ mm}$ .

Optimization of the compression stage was conducted with the one-dimensional 3T code DEIRA (Basko, 1990) in cylindrical geometry. The beam heating was simulated as a prescribed specific deposition power,

$$q_{cb}(t, r) = I_{cb}(t, r) \frac{S(t, r)}{\rho_a(t, r) E_{i0}} [\text{erg g}^{-1} \text{ s}^{-1}], \quad (1)$$

confined to an annular region  $r_{b1} \leq r \leq r_{b2}$ , where  $r_{b1} > R_{DT,0}$  and  $r_{b2} < R_0$ . Here  $I_{cb}(t, r)$  [ $\text{W/cm}^2$ ] is the intensity of irradiation,

$$S(t, r) = \left| \frac{dE_i}{dz} \right| \quad (2)$$

is the  $z$ -averaged value of the stopping power (in one-dimensional simulations we simply evaluated it at given  $t$  and  $r$  for a fixed ion energy  $E_i = E_{i0}$ ), and  $\rho_a(t, r)$  is the current value of the absorber density. The radial profile of the irradiation intensity,

$$I_{cb}(t, r) = \frac{W_{cb}(t)}{\pi(r_{b2}^2 - r_{b1}^2)} \frac{3}{2} \left[ 1 - \left( \frac{2r - r_{b1} - r_{b2}}{r_{b2} - r_{b1}} \right)^2 \right], \quad (3)$$

was chosen as an inverted parabola subtending the interval  $r_{b1} \leq r \leq r_{b2}$ ;  $W_{cb}(t)$  [W] is the total power of the compression beam.

In the process of optimization, we tried to minimize the total beam energy

$$E_{cb} = 2\pi \iint I_{cb}(t, r) r dr dt = \int W_{cb}(t) dt. \quad (4)$$

In doing so, we assumed that this energy was used to compress a cylinder section with a fixed length  $L = E_{i0}/S_0$ , where  $S_0$  is the stopping power (2) at  $t = 0$ . Then, the beam losses due to the absorber clearance can be characterized by the efficiency coefficient

$$\eta_{clr} = \frac{E_{cb,dep}}{E_{cb}} \leq 1, \quad (5)$$

where

$$\begin{aligned} E_{cb,dep} &= 2\pi L \iint q_{cb}(t, r) \rho_a(t, r) r dr dt \\ &= 2\pi \iint I_{cb}(t, r) \left[ \frac{S(t, r)}{S_0} \right] r dr dt \end{aligned} \quad (6)$$

is the total energy actually deposited in the cylinder over the length  $L$ . Note that under our conditions, the stopping power per unit mass coordinate,  $S(t, r)/\rho_a(t, r)$ , is nearly constant, and to a good accuracy

$$\frac{S(t, r)}{S_0} \approx \frac{\rho_a(t, r)}{\rho_{a0}}. \quad (7)$$

In simulations, we used the value  $E_{i0} = 125 \text{ GeV}$  for  $\text{Bi}^{209}$  ions, which corresponds to  $L = 1.31 \text{ cm}$  in lead at normal conditions ( $\rho_{a0} = 11.3 \text{ g/cm}^3$ ).

We found that we need at least  $dE_{cb,dep}/dz = 6.53 \text{ MJ/cm}$  of the deposited energy to compress the DT fuel to the required  $\rho_{DT} = 100 \text{ g/cm}^3$ ,  $R_{DT} = 50 \text{ }\mu\text{m}$ . In the best case, we obtained the clearance coefficient  $\eta_{clr} = 0.65$ . The latter means that we need at least  $E_{cb} = E_{cb,dep}/\eta_{clr} = 10 \text{ MJ}$  in the compression beam for a 1-cm-long target. If allowance should be made for letting the Bragg peak be outside the working target section, this value should additionally be multiplied by  $\eta_z^{-1}$ , where, presumably,  $\eta_z \approx 0.65\text{--}0.75$ .

The optimal pulse profile for the total beam power  $W_{cb}(t)$  (per 1 cm of the target length) is shown in Figure 3. The entire pulse consists of a 20-ns-long prepulse and the main pulse at  $44 \text{ ns} < t < 75 \text{ ns}$ . The peak power at  $65 \text{ ns} < t < 75 \text{ ns}$  is  $525 \text{ TW/cm}$ . In the process of optimization, we found that it is advantageous to use a larger focal area for the prepulse compared with the main pulse: This allows us to minimize the radial expansion of the absorber prior to the main pulse and, consequently, achieve higher values of  $\eta_{clr}$ . In the optimal case, the inner radius of the beam deposition area,  $r_{b1} = 1.22 \text{ mm}$ , was the same for the entire pulse, whereas its outer radius was  $r_{b2} = 3.62 \text{ mm}$  in the prepulse, and  $r_{b2} = 2.52 \text{ mm}$  in the main pulse.

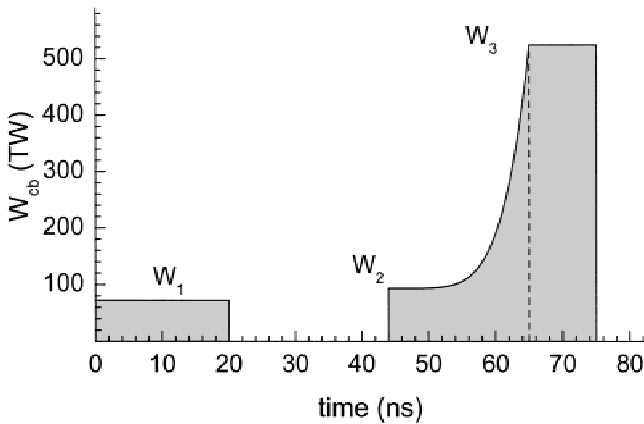


**Fig. 3.** Optimized pulse shape of the compression beam. Absolute power  $W_{cb}(t)$  is normalized to a 100% beam absorption at  $t = 0$  in a 1-cm-long lead absorber.

For efficient compression, we have to keep the fuel entropy as low as possible. The prepulse launches a 1-Mbar first shock in the DT ice. The second shock, launched by the main pulse, catches up with the first one just after the latter rebounds from the target axis. The final phase of compression is accomplished by the heavy (lead) pusher converging towards the axis with a relatively low implosion velocity peaking at  $4.6 \times 10^6$  cm/s. Figure 4 shows the radial profiles of the density and the entropy parameter  $\alpha = P/P_{deg}$  in the compressed target core at stagnation ( $t = 93.76$  ns); here  $P_{deg} = 2.18\rho^{5/3}$  [Mbar] is the fully degenerate pressure of the ideal electron gas in DT at a density  $\rho$  [g/cm<sup>3</sup>]. One sees that most of the fuel mass stagnates at a very low fuel entropy corresponding to  $\alpha \lesssim 1.5$ .

#### 4. CONCLUSION

Direct drive cylindrical targets may become a feasible target option if preference should be given to a heavy-ion driver with energetic ions, which have long ( $\approx 10$  g/cm<sup>2</sup>) ranges in matter. Our preliminary analysis reveals that the minimum beam energy, required for cold compression of the DT fuel, lies in the range 10–15 MJ/cm. Ignition and axial burn propagation can be achieved by applying a second high-power ion pulse of duration 0.2 ns with the beam energy of 0.4 MJ. Although we do not have reliable two-dimensional calculations of the overall burn fraction  $f_b$ , one-dimensional results indicate that the values as high as  $f_b \approx 0.4$ –0.6 can be obtained. Then, one can count on target energy gains in the range  $G = 50$ –150.

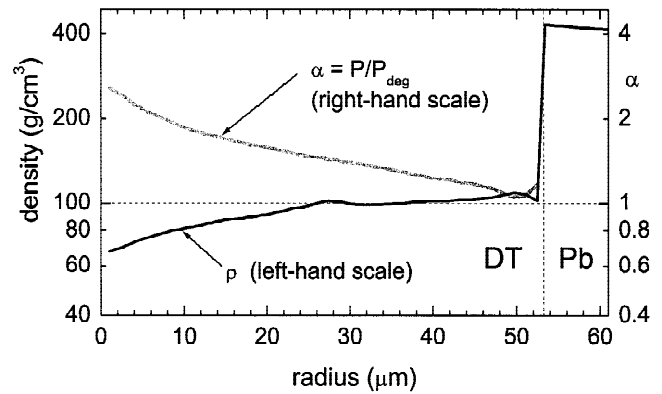


**Fig. 4.** Radial profiles of the density and the entropy parameter  $\alpha = P/P_{deg}$  in the compressed target core at stagnation.

In this target, once an adequate azimuthal and axial uniformity of beam irradiation is ensured, the Rayleigh–Taylor instability of the cold heavy pusher becomes an important issue, which has not been addressed in this work. The instability at the absorber–pusher interface during the acceleration phase can, in principle, be mitigated by a smooth density gradient (Basko *et al.*, 2002). The role of the instability and turbulent mixing at the pusher–fuel interface during the deceleration phase should be thoroughly addressed in the future studies of this type of targets.

#### REFERENCES

- ATZENI, S. (1999). Inertial fusion fast ignitor: Igniting pulse parameter window vs the penetration depth of the heating particles and the density of the precompressed fuel. *Phys. Plasmas* **6**, 3316–3326.
- AVRORIN, E.N., BUNATYAN, A.A., GADJIEV, A.D., MUSTAFIN, K.A., NURBAKOV, A.SH., PISAREV, V.N., FEOKTISTOV, L.P., FROLOV, V.D. & SHIBARSHOV, L.I. (1984). Numerical simulations of thermonuclear detonation in a dense plasma. *Sov. J. Plasma Phys.* **10**, 298–303.
- BASKO, M.M., MARUHN, J.A. & SCHLEGEL, T. (2002). Hydrodynamic instability of shells accelerated by direct ion beam heating. *Phys. Plasmas* **9**, 1348–1356.
- BASKO, M.M. (1990). Spark and volume ignition of DT and DD microspheres. *Nucl. Fusion* **30**, 2443–2452.
- CHURAZOV, M.D., AKSENOV, A.G. & ZABRODINA, E.A. (2001). Ignition of thermonuclear targets by a beam of heavy ions. *Voprosy Atomnoi Nauki i Tekhniki*, ser.: Matem. Model. Fiz. Protsessov, vyp. 1, 20–28.
- VATULIN, V. (2002). Numerical modeling of forthcoming experiments on TWAC. Invited talk at the 14th Int. Symp. on Heavy Ion Inertial Fusion, May 26–31, 2002, Moscow, Russia.